Energy Conversion and Management 248 (2021) 114798

Contents lists available at ScienceDirect

Energy Conversion and Management

journal homepage: www.elsevier.com/locate/enconman

A hybrid indirect evaporative cooling-mechanical vapor compression process for energy-efficient air conditioning

Qian Chen [a,*], M. Kum Ja [a], Muhammad Burhan [a], Faheem Hassan Akhtar [a], Muhammad Wakil Shahzad [a,b], Doskhan Ybyraiymkul [a], Kim Choon Ng [a]

[a] Water Desalination and Reuse Center, King Abdullah University of Science and Technology, Thuwal 23955, Saudi Arabia
[b] Northumbria University, Newcastle UPON Tyne, United Kingdom

ARTICLE INFO

Keywords:
Indirect evaporative cooler
Mechanical vapor compression
Room exhaust air
Energy recovery

ABSTRACT

The indirect evaporative cooler (IEC) is deemed an effective and sustainable alternative to existing mechanical vapor compression (MVC) chillers in cooling applications. However, IEC is a passive cooler that has no effective control over the supply air temperature and humidity. Also, the performance of IEC degrades severely when the humidity of the air is high. To overcome these limitations, we investigate a hybrid process that connects IEC and MVC in tandem. The outdoor air is firstly pre-cooled in the IEC by recovering energy from the room exhaust air, and then it is further processed to the desired condition using MVC. Such a hybrid IEC-MVC process benefits from IEC's high energy efficiency and MVC's capability of humidity and temperature control. A pilot IEC unit with the cross-flow configuration is firstly constructed and tested under assorted outdoor air conditions. Employing the room exhaust air as the working air in the wet channels, the IEC simultaneously cools and dehumidifies the outdoor air. Under the operating conditions considered, the outdoor air temperature can be reduced by 6–15 °C, and the humidity ratio drops by 0.5–4 g/kg. The coefficient of performance (COP) for IEC is 6–16, leading to an overall COP of 4.96–6.05 for the hybrid IEC-MVC process. Compared with a standalone MVC, the electricity consumption can be reduced by 19–135%.

1. Introduction

With the increase of global energy consumption for air conditioning (AC) [1,2], searching for energy-efficient and environmentally-friendly cooling technologies is becoming more and more critical. The indirect evaporative cooler (IEC) is an effective and sustainable alternative to existing mechanical vapor compression (MVC) systems in cooling applications [3]. It uses the evaporation of water as a natural driving force, and the energy consumption is very low [4]. Therefore, IEC has been the subject of great research interests.

One important research direction for IEC is the development of mathematical models for performance prediction and optimization. Dizaji et al. [5] presented a novel mathematical model for a regenerative IEC based on the wet-surface theory. The model can generate the distribution of temperature and humidity ratio along the dry and wet channels. Cui et al. [6] developed a non-dimensional correlation for a counter-flow regenerative IEC, which offers a practical approach for performance prediction. Heidarinejad and Moshari [7] proposed a mathematical model considering wall longitudinal heat conduction and spray water temperature. The model showed a small error of 3% when compared with experimental data. Cui et al. [8] developed a modified log mean temperature difference (LMTD) method, and it allows for quick evaluation of IEC performance. Anisimov, Pandelidis, and Danielewicz [9] developed numerical models for five IEC configurations based on the modified ε-NTU (number of transfer units) method. The models revealed many novel characteristics of the proposed configurations. Zhu, Chow and Lee [10] developed a data-driven model based on the artificial neural network algorithm. The discrepancy between the predicted temperature drop and the experiment measurement was 5%.

Based on analytical or experimental methods, several strategies have been proposed to optimize the cooling performance of IEC. Li et al. [11] compared the performance of vertical and horizontal IECs. Under the same operation conditions, the vertical IEC was found to have 24–44% higher cooling capacity. Cui et al. [12] proposed to install artificial ribs in the dry and wet channels to enhance heat and mass transfer. The wet-bulb effectiveness can be improved by 10–20%. Duan et al. [13] tested a counter-flow regenerative IEC considering the effect of water

* Corresponding author.
E-mail address: chen_qian@u.nus.edu (Q. Chen).

https://doi.org/10.1016/j.enconman.2021.114798
Received 29 July 2021; Accepted 21 September 2021
Available online 29 September 2021

Nomenclature

Abbreviations

AC	Air conditioning
CMH	Cubic meter per hour
COP	Coefficient of performance
IEC	Indirect evaporative cooler
LMTD	Log-mean temperature difference
MVC	Mechanical vapor compression
NTU	Number of transfer units

Symbols

$\dot{Q}$	Cooling load, W
h	Specific enthalpy, J/kg
$\dot{m}$	Mass flowrate, kg/s
min	Minimum
W	Electricity consumption, W
X	Cooling load ratio, %

Greek letters

ε	Effectiveness, %
η	Efficiency, %
ω	Humidity ratio, g/kg

Subscripts

comp	Compressor
cond	Condensation
evap	Evaporation
fan	Fan
ma	Mixed air
oa	Outdoor air
pump	Pump
r	Refrigerant
s	Isentropic; saturation

temperature. A lower water temperature was found to promote the cooling performance. Al-Zubaydi and Hong [14] studied the effect of water spray mode on the performance of IEC. The mixed internal-external spray mode achieved the highest wet-bulb effectiveness, cooling capacity, and coefficient of performance (COP). Ali et al. [15] employed aluminum fins in IEC dry channels to improve heat and mass transfer, which increased the cooling capacity by 18%.

Several advanced IEC designs have also emerged. Moshari, Heidarinejad and Fathipour [16] proposed several types of IECs with two-stage configuration. The wet-bulb effectiveness can be increased to 91%, as compared to 60% for the single-stage IEC. Muhammad et al. [17,18] designed a generic-cell IEC unit with multi-point working air injection. It can produce more than 10 °C of temperature drop within a small area. Jradi and Riffat [4] fabricated an IEC using the psychometric energy core. Under an intake air temperature of 30 °C and relative humidity of 50%, the system attained wet-bulb effectiveness of 112%. Wan et al. [19] proposed a novel counter-flow closed-loop IEC configuration, and it could achieve the simultaneous goals of pre-cooling, energy recovery, and dehumidification. Heidarinejad and Moshari [7] numerically compared several IEC configurations. The two-stage IEC was found to have 50% higher wet-bulb effectiveness than the one-stage IEC. Duan et al. [20] designed and fabricated a novel counter-flow regenerative IEC using stacked sheets composed of high wicking evaporation and water-proof aluminum materials. It demonstrated better cooling performance than existing IEC designs. Fikri, Sofia and Putra [21] designed an IEC incorporated with heat pipes. The largest temperature drop of the process air was observed to be 18.15 °C. Wang et al. [22] fabricated an IEC unit using novel porous ceramics material, which has high hydrophilicity and water storage capability. The unit achieved a high COP of 34.9.

A critical limitation of IEC is that its performance degrades severely when the air has high humidity. To achieve the desired cooling performance, the humid air has to be dehumidified before entering IEC. Heidari et al. [23] and Pandelidis et al. [24] presented the combination of IEC with desiccant wheels, and Cui et al. [25,26] evaluated the combined liquid desiccant-IEC system. However, the energy efficiency of these systems is very low, as the COP of most dehumidifiers is lower than 1 [27,28]. To achieve better cooling performance, researchers have looked into the combination of IEC with MVC. The hybrid system uses IEC as a pre-cooler to reduce the cooling load of MVC, thus reducing the overall electricity consumption. Another advantage is that IEC can use room exhaust air, which is colder and drier than the outdoor air, as the working air in the wet channels to boost IEC performance.

Several studies have been reported to combine IEC with MVC. Duan et al. [29] evaluated the energy-saving potential of the hybrid IEC-MVC system under the climatic condition of Beijing, China. Compared with a standalone MVC, the hybrid system demonstrated a seasonal energy saving of 38.2%. Delfani et al. [30] studied the performance of the hybrid IEC-MVC system in four cities of Iran. IEC could reduce the cooling load and electricity consumption by 75% and 55%, respectively. Zanchini and Naldi [31] experimentally evaluated the energy-saving potential of the hybrid IEC-MVC system for an office building in North Italy. The total electricity consumption is 38% lower. Cui et al. [32,33] presented an experimental and analytical study of a hybrid IEC-MVC system under the climatic conditions of Singapore. IEC can reduce the cooling load of MVC by 32%. Chen et al. [34,35] conducted a numerical study on IEC that works as a pre-cooler of MVC. Results revealed that the channel gap and the cooler height had the most influence on the cooling performance. Min, Chen and Yang [36] developed a statistical modeling approach for IEC based on training data extracted from a 2-D model [37]. The model was able to predict the wet-bulb efficiency within a 9.52% deviation.

Table 1 summarizes existing studies on the hybrid IEC-MVC process. It can be seen that the hybrid process is still at an undeveloped stage with several research gaps. Firstly, most of the existing studies are based on the climatic data of a specific area, and there is no systematic evaluation of the system performance that covers different weather conditions. Secondly, as IEC operates with room exhaust air in the wet channels, there is simultaneous cooling and dehumidification in the dry

Table 1
Summary of existing studies on the hybrid IEC-MVC process.

Source	Method	Highlights
Duan et al. [29]	Simulation	Dynamic simulation of seasonal energy-saving potential under the climatic condition of Beijing, China;
Delfani et al. [30]	Experiment	Experimentally evaluating the energy-saving potential for four cities in Iran;
Zanchini and Naldi [31]	Experiment	Experimental evaluation of energy-saving for an office in North Italy;
Cui et al. [32,33]	Simulation	Analytical study of IEC as the pre-cooler under the climatic condition of Singapore;
Chen et al. [34,35]	Simulation	Sensitivity study on the impacts of key parameters on IEC performance;
Min et al. [36]	Simulation	Development of a statistical model for an air-conditioning system using IEC for heat recovery;
Current study	Experiment and simulation	Experimental study of the IEC operating with room exhaust air in the wet channels; Evaluation of energy-saving potential of IEC-MVC under a wide range of outdoor air conditions;

channels, making the system behavior different from that in a regular IEC. However, most of the existing studies on such a process are based on numerical simulation, and there is a lack of experimental investigation.

This study is intended to conduct a systematic investigation of the hybrid IEC-MVC process. Firstly, the performance of IEC as a pre-cooler of MVC will be experimentally evaluated under various climatic conditions. Secondly, the effectiveness of energy recovery from room exhaust air will be explored, and a simplified correlation will be developed for quick performance prediction. Thirdly, the energy-saving potential of the hybrid IEC-MVC process over the standalone MVC will be quantified. To achieve these objectives, a pilot IEC unit will be fabricated and tested under assorted temperatures, humidity ratios, and flowrates of outdoor air. Based on the experimental data, the energy-saving potential of the hybrid IEC-MVC process will be predicted and compared with that of a standalone MVC under different climatic conditions. The derived results will provide useful information for future installation of the hybrid IEC-MVC system. The rest of this paper is organized as follows. Section 2 briefly describes the working principles of the hybrid IEC-MVC process, and Section 3 presents the experimental setup and the analytical model. Section 4 discusses the energy recovery performance of IEC and the energy-saving potential of the hybrid IEC-MVC system. Finally, key findings and conclusions are summarized in Section 5.

2. System description

Fig. 1 shows the schematic of the combined IEC-MVC system, which treats outdoor air with high temperature and humidity. The outdoor air (1) enters the dry channels of IEC. Simultaneously, the room exhaust air (4), which is cold and dry, flows through the wet channels to cool down the outdoor air stream in the dry channels. The wet channels are supplied with water, which evaporates and absorbs heat from the air to further cool down the outdoor air. When the temperature in the dry channels is lower than the dew-point temperature of the outdoor air, condensation occurs, and the humidity ratio of the outdoor air drops. The pre-cooled and dehumidified outdoor air (2) is then passed through the evaporator coils of a mechanical chiller to further bring down its temperature and humidity to the desired values. Meanwhile, the exhaust air (5) leaving the wet channels is mixed with outdoor air (1′) and channeled to the condenser for heat rejection.

Fig. 2 demonstrates the above-mentioned processes in the psychometric chart. The room exhaust air (4) is simultaneously heated and humidified in the wet channels of the IEC, which recovers both the sensible and latent energy for pre-cooling and dehumidifying the outdoor air. The exhaust air leaving the wet channels (5) is still colder than the outdoor air and is used as part of the cooling media of the MVC condenser to recover its cooling potential further. In this manner, the sensible and latent potential of the room exhaust air is effectively reused, which will significantly reduce the overall energy consumption.

3. Methodology

The energy-saving potential of the proposed system is evaluated experimentally and analytically. A 1-Rton IEC unit is firstly designed and commissioned to quantify the effectiveness of energy recovery from the room exhaust air. Afterward, the overall energy consumption of the hybrid IEC-MVC process is analyzed and compared with that of standalone MVC.

3.1. IEC experiment design

A 1-Rton IEC unit is designed and commissioned in the Water Desalination and Reuse Center, King Abdullah University of Science and Technology (KAUST). A pictorial view of the unit is shown in Fig. 3(a). The unit has a cross-flow configuration with a dimension of 1 m × 1 m × 0.7 m. 200 mm × 300 mm chamfers are cut at the four corners to form the entrances and exits of dry and wet channels. The air flow channels are connected to acrylic ducts. At the inlet of the wet channels, two rows of spray nozzles are installed to supply fine water droplets. Fig. 3(b) shows the heat and mass exchanger in the unit. It consists of 50 dry channels and 50 wet channels arranged in an alternating manner. The channel walls are made of aluminum plates with a thickness of 300 μm. These plates are separated with spacers (5 mm thickness) to form the flow channels.

During operation, the room air is directly supplied to the wet channels, while an environmental test chamber (PAU-A1400S-HC) is used to supply air to the dry channels. The environmental chamber can provide air at different temperatures (20–35 °C, ±0.2 °C accuracy) and humidity

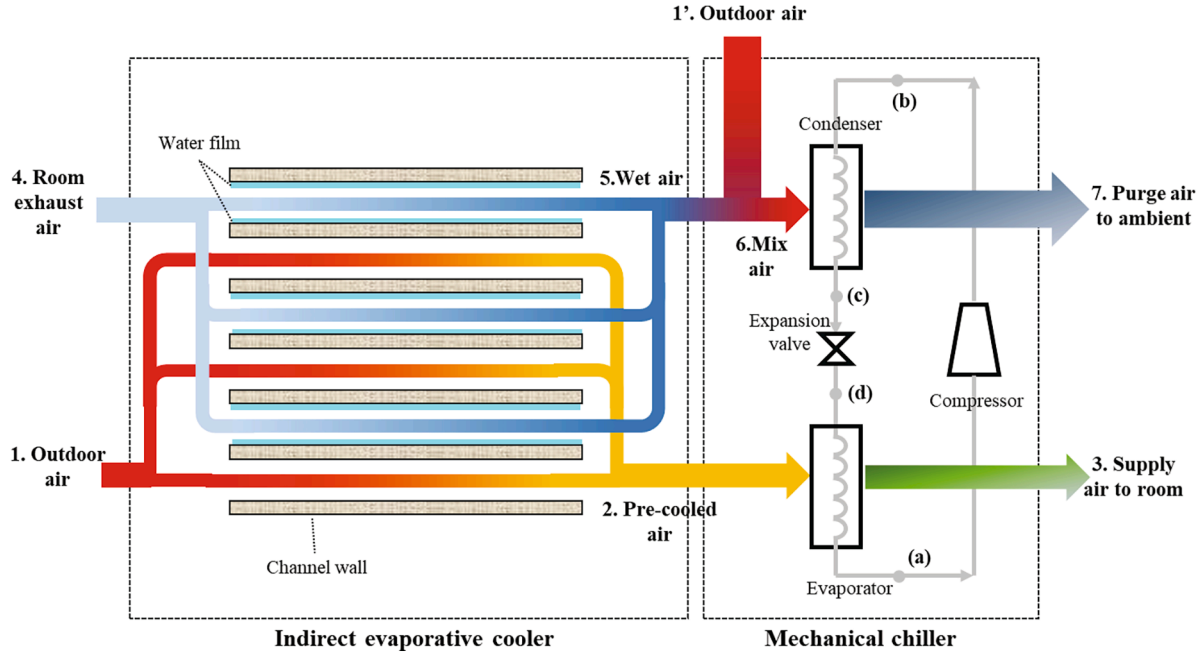

Fig. 1. Schematic of the combined IEC-MVC system.

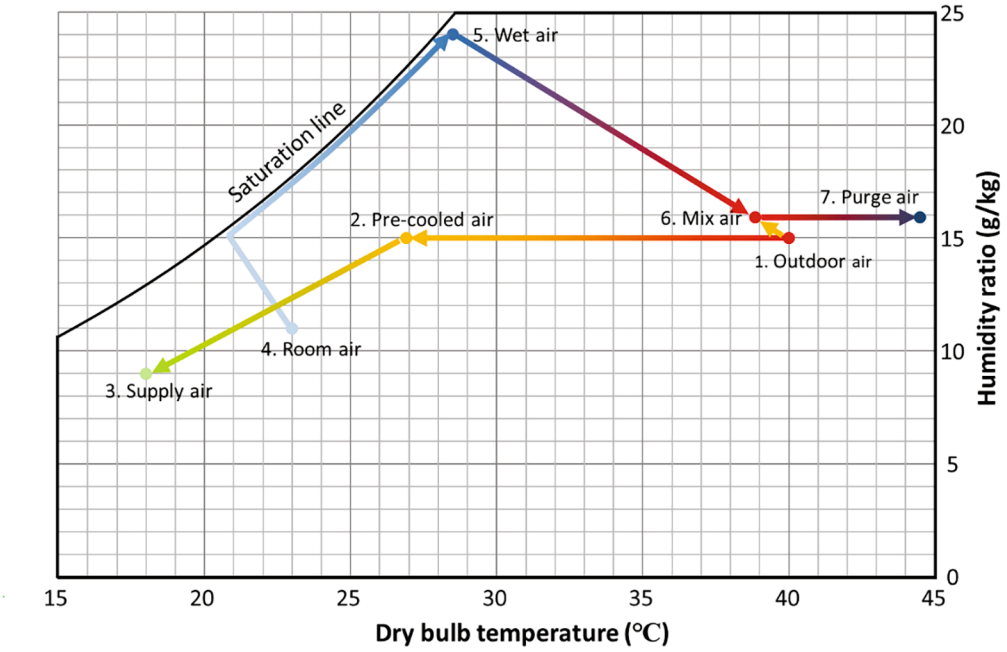

Fig. 2. Process demonstration of the combined IEC-MVC system in psychometric chart.

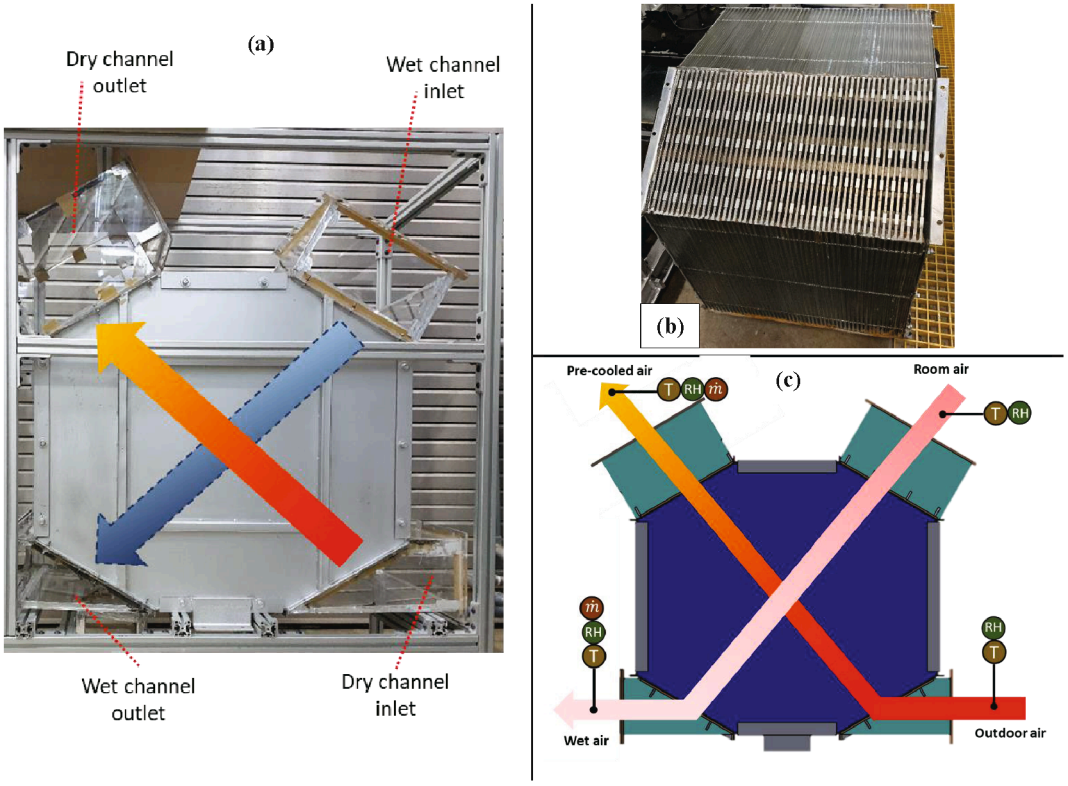

Fig. 3. (a) Photo of the 1-Rton IEC unit at KAUST, (b) the heat and mass exchanger, and (c) schematic of the experimental setup.

(RH 40–80%, ±1% accuracy), which allows the simulation of different outdoor conditions. A 2000 W hot air gun is placed after the environmental chamber to increase the air temperature further. The temperature and humidity of the air streams are measured using thermistors (TJ36-44004–1/8–12, OMIGA) as well as temperature/humidity probes (FH400, Degree Controls Inc.). The flowrates of air are measured using air orifices, which correlate the air flowrate to the pressure drop across the nozzle. Fig. 3(c) shows the schematic of sensor arrangements, and Table 2 summarizes the technical specifications of the sensors.

3.2. MVC modelling

The performance of MVC is analyzed based on energy balance in each component. Referring to the state points shown in Fig. 1, energy

Table 2
Technical data of measurement instrumentations.

Parameter	Sensor	Range	Accuracy
Temperature	TJ36-44004–1/8–12, OMIGA	0–60 °C	±0.1 °C
Temperature	FH400, Degree Controls Inc.	20–60 °C	±0.2 °C
Relative humidity	FH400, Degree Controls Inc.	10–90%	±2%
Pressure drop	2600 T Series Pressure Transmitter, ABB	0–400 Pa	± 5 Pa

conservation in the evaporator is expressed as

$$\dot{Q}_{evap} = \dot{m}_{oa}[h(T_2, \omega_2) - h(T_3, \omega_3)] = \dot{m}_r(h_a - h_d) \quad (1)$$

where $\dot{Q}_{evap}$ is the heat transfer rate in the evaporator; $\dot{m}_{oa}$ and $\dot{m}_r$ are the flowrates of outdoor air and refrigerant, respectively; h is the specific enthalpy and ω is the humidity ratio of air.

Similarly, the energy balance of the condenser is expressed as

$$\dot{Q}_{cond} = \dot{m}_{ma}[h(T_7, \omega_7) - h(T_6, \omega_6)] = \dot{m}_r(h_b - h_c) \quad (2)$$

The compression process is modelled by considering the isentropic compression efficiency

$$\eta_{comp} = \frac{h_{b,s} - h_a}{h_b - h_a} \quad (3)$$

$$W_{comp} = \dot{m}_r(h_b - h_a) \quad (4)$$

where $h_{b,s}$ is the specific enthalpy of the refrigerant at the exit of isentropic compression, η_{comp} is the isentropic efficiency and W_{comp} is the compressor power input.

The throttling valve is an isothermal device, and its energy balance is expressed as

$$h_d = h_c \quad (5)$$

3.3. Performance indicators

The performance of IEC is firstly evaluated by the effectiveness of enthalpy recovery

$$\varepsilon = \min\{\frac{h_1 - h_2}{h_1 - h_{2,s}}, \frac{h_5 - h_4}{h_{5,s} - h_4}\} \quad (6)$$

where $h_{2,s}$ is the enthalpy of the outdoor air when it is cooled down to the same temperature as the room purge air, while $h_{5,s}$ is the enthalpy of the purge air when it reaches the same temperature as the outdoor air with 100% relative humidity.

Another important parameter for IEC is the coefficient of performance (COP), which is the ratio of the cooling effect to the electricity consumption

$$COP_{IEC} = \frac{\dot{m}_{oa}(h_1 - h_2)}{W_{pump} + W_{fan}} \quad (7)$$

where W_{pump} and W_{fan} are the electricity consumption of the spray pump and the fans, respectively.

Similarly, the performances of MVC and IEC-MVC are also quantified by their COPs

$$COP_{MVC} = \frac{\dot{Q}_{evap}}{W_{comp}} \quad (8)$$

$$COP_{IEC-MVC} = \frac{\dot{m}_{oa}(h_1 - h_3)}{W_{comp} + W_{pump} + W_{fan}} \quad (9)$$

In addition to COP, we also evaluate the percentage of cooling load that can be provided by the IEC unit, as it helps to quantify the energy-saving potential of using IEC as the pre-cooler. The ratio of cooling load undertaken by IEC is calculated as

$$X_{IEC} = \frac{\dot{Q}_{IEC}}{\dot{Q}_{total}} = \frac{\dot{m}_{oa}(h_1 - h_2)}{\dot{m}_{oa}(h_1 - h_3)} \quad (10)$$

4. Results and discussion

This section discusses the performance of the proposed process. The energy recovery performance of the IEC unit is firstly evaluated experimentally. Then the energy efficiency of the hybrid IEC-MVC process is analyzed and compared with that of a standalone MVC.

4.1. IEC performance

Employing the experimental setup, the energy recovery performance of the IEC is evaluated. Hot and humid air, provided by the environmental chamber, is supplied to the dry channels to simulate the outdoor air. Its temperature is ranged between 30 and 42 °C, and the humidity ratio is 10–20 g/kg. The wet channel is supplied with room air, which has a temperature of 23 ± 1 °C and a humidity ratio of 11 ± 1 g/kg. The air flowrate in the dry channels is varied between 280 and 420 CMH by controlling the fan speed, while that in the wet channels is fixed at 230 CMH. The parameter setting is summarized in Table 3.

Fig. 4 shows the temperature profiles of air entering and leaving the IEC during one set of experiments. The humidity ratio of the outdoor air is fixed at 15 g/kg, while the room air condition is 23.5 °C and 10.5 g/kg. With the step-wise increment of the outdoor air temperature, the air temperatures leaving the dry and wet channels increase accordingly. After the outdoor air temperature is stabilized, it takes another 1000 s for the exiting temperatures to reach a steady state (i.e., temperature change over 10 min is < 0.1 °C). The outdoor air temperature drops by 11–14 °C in the dry channels, and the wet channel air temperature is always ~ 2.5 °C higher than that in the dry channels. It should be noted that the wet-bulb air temperature in the wet channels is almost the same as its dry-bulb temperature. In other words, the air in the wet channels is fully saturated when leaving the wet channels, indicating effective recovery of the latent potential from the room exhaust air.

Fig. 5(a-b) shows the change of outdoor air temperature and humidity ratio in the dry channels under different outdoor air temperatures. Each data point is the average value of more than 3 measurements. For each measurement, the value is recorded after the temperatures are stabilized for more than 600 s, as previously shown in Fig. 4. Under a constant humidity ratio, the changes in temperature and humidity ratio are linearly proportional to the outdoor air temperature. This is consistent with the observations reported in the literature [33,38]. The reason can be explained as follows. When the outdoor air temperature is higher, the exhaust air in the wet channels can be heated to a higher temperature, which provides more sensible cooling effects. More importantly, a higher air temperature in the wet channels increases the saturation humidity ratio and allows more evaporation, leading to more latent cooling effects. The enhanced sensible and latent cooling effects result in a larger drop of temperature and humidity ratio in the dry channels. The temperature drop is in the range of 6–15 °C. When the outdoor air temperature is low at 31 °C, it can be pre-cooled to ~ 23 °C, which is very close to the desired supply air temperature (18–20 °C). In this case, the IEC is able to undertake the majority of the sensible cooling

Table 3
Ranges of experimental parameters.

Parameter	Range
Outdoor air temperature (°C)	30–42
Outdoor air humidity ratio (g/kg)	13–20
Outdoor air flowrate (CMH)	280–420
Exhaust air temperature (°C)	23 ± 1
Exhaust air humidity ratio (g/kg)	11 ± 1
Exhaust air flowrate (CMH)	230

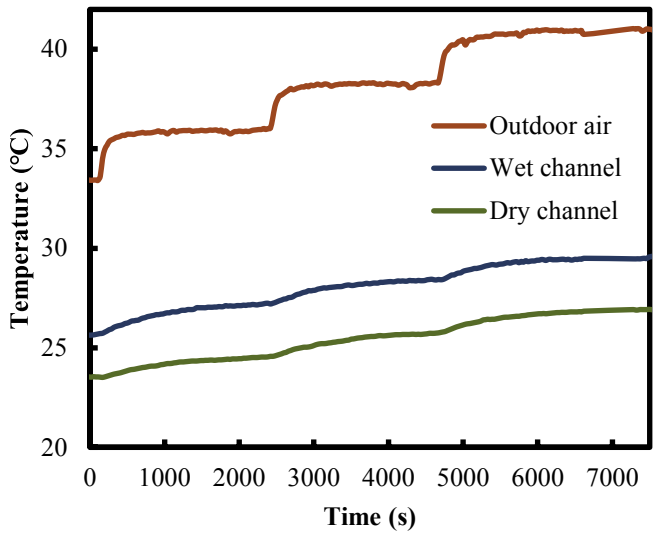

Fig. 4. Temperature profiles for air streams entering and leaving IEC.

load, and the MVC only needs to handle the latent load.

Fig. 5(c-d) shows the drop of outdoor air temperature and humidity ratio under varying outdoor humidity ratios. When the outdoor humidity is high, there is more potential for condensation, and the drop of air humidity in the dry channels is larger, as can be seen from Fig. 5(d). With more moisture condensation in the dry channels, more condensation heat is released, which heats up the air in both dry and wet channels. Consequently, the air temperature drop in the dry channels is smaller, as shown in Fig. 5(c). When the outdoor air humidity ratio is low at 13.46 g/kg, IEC is able to bring down the humidity to ~ 11 g/kg, a value that is close to the room air humidity. In other words, IEC handles most of the latent load by recovering energy from the room exhaust air.

Fig. 5(e-f) shows the effect of dry channel air flowrate on the changes in temperature and humidity ratio. The air flowrate in the wet channels is fixed at 230 CMH. When the air flowrate in the dry channels increases from 280 to 350 CMH, the drops of temperature and humidity ratio become less significant. The reason is that the total amount of cooling capacity is fixed under a given wet channel air flowrate. Therefore, the higher the dry channel air flowrate, the smaller the enthalpy change for the unit mass of air. When further increasing the air flowrate from 350 to 420 CMH, the descending trend of temperature change remains, while the humidity change is slightly higher. This is attributed to the improvement of heat and mass transfer coefficients under a higher air flowrate in the dry channels.

As there are simultaneous heat and mass transfer in the dry channels, the enthalpy exchange effectiveness and COP (defined by *Eqs.6&7*) allow better measurement of the IEC performance, as they account for both temperature and humidity change. Fig. 6(a-b) shows the enthalpy recovery effectiveness and COP of IEC under different outdoor air temperatures. As defined, the enthalpy recovery effectiveness is the ratio of actual enthalpy transfer to maximal possible enthalpy transfer. When the outdoor temperature is higher, the available cooling potential is also higher, while the IEC unit is unable to completely recover such potential due to a limited surface area for heat and mass transfer. As a result, the effectiveness is lower at a higher outdoor temperature, as revealed by Fig. 6(a). The COP, in contrast, is higher when the outdoor temperature is higher, as plotted in Fig. 6(b). With a higher outdoor air temperature, there is a larger drop of temperature and humidity in the dry channels, providing more cooling effects. On the other hand, the energy consumption for the fans and the water pump is fixed with the air flowrate. Thus, the higher the outdoor temperature, the higher the COP is. The COP is in the range of 8–14, despite a high outdoor humidity ratio of 20 g/kg. Such a high COP value is the result of effective sensible and latent heat recovery from the room exhaust air.

Fig. 6(c-d) presents the effect of the outdoor humidity ratio on IEC effectiveness and COP. Different from the effect of temperature, a higher humidity ratio leads to higher energy recovery effectiveness. This is mainly because higher outdoor humidity induces more condensation, which significantly enhances heat and mass transfer in the dry channels [39]. The COP is also higher when the outdoor humidity ratio is higher, as there is not only higher cooling potential but also more effective energy recovery.

A higher air flowrate also promotes heat and mass transfer coefficients and leads to higher IEC effectiveness, as plotted in Fig. 6(e). With the increase of dry channel air flowrate from 280 to 420 CMH, the effectiveness can be increased by 4%, regardless of the outdoor humidity ratio. Fig. 6(f) shows the change COP with flowrate, which demonstrates a different trend from the effectiveness. It firstly decreases when increasing the air flowrate from 280 to 350 CMH, while further increasing the flowrate to 420 CMH leads to a higher COP. This is attributed to several competing effects when increasing the flowrate. On the one hand, a higher flowrate reduces the total cooling potential for the dry channels and causes the decrease of COP, as addressed previously. On the other hand, heat and mass transfer are promoted under a higher air flowrate, which allows for better recovery of the cooling potential. The trend of COP change with flowrate is the result of the trade-off between these two effects.

To enable a quick prediction of the energy recovery performance, we use the multi-variable regression method to correlate the IEC effectiveness with the operating parameters, including the temperature and humidity ratio of the outdoor and room air, as well as the air flowrate ratio between the dry and the wet channels. The regression is performed using the Constraint Multiple Regression app embedded in OriginPro [40]. 88 measurement points were included, and the coefficient of determination (R^2) for the regression is 0.95. Details of the fitting results for each parameter are summarized in Table 4.

Based on the regression results, the IEC effectiveness is correlated to the operating variables in *Eq.11*. The dashed lines in Fig. 6(a), (c) and (e) are the effectiveness calculated by *Eq.11*, which adhere closely to the experimental data. The fitting equation will be used to predict the energy-saving potential of IEC in the next sub-section.

$$\varepsilon = 0.416 - 5.81 \times 10^{-3} T_{OA} + 4.65 \times 10^{-3} \omega_{OA} + 1.42 \times 10^{-3} T_{RA} - 5.65 \times 10^{-3} \omega_{RA} + 7.49 \times 10^{-4} \frac{\dot{m}_{oa}}{\dot{m}_{ra}} \quad (11)$$

4.2. Energy saving potential

Based on the experimental results on IEC, we compare the COP of the hybrid IEC-MVC process with that of standalone MVC. The effectiveness of energy recovery from IEC is firstly calculated using *Eq.11*. Then, the energy consumption to further cool down the outdoor air to the supply condition (3) is calculated via *Eqs.1–5*. For comparison purposes, the energy consumption of a standalone air-cooled MVC chiller, which directly cools down the outdoor air to the supply condition (from 1 to 3), is also calculated. For both systems, the isentropic efficiency (η_{comp} in

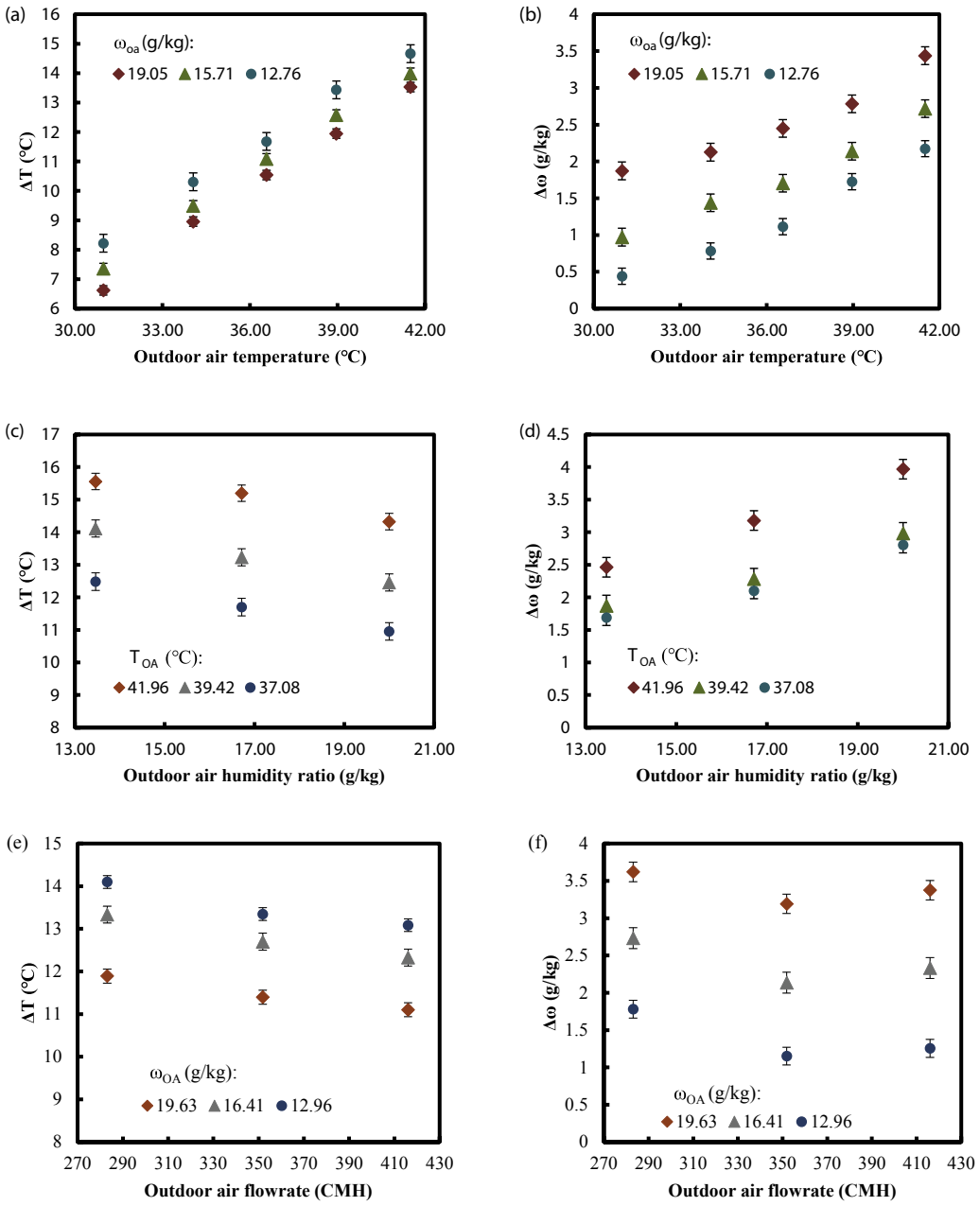

Fig. 5. Air temperature and humidity drop in dry channels under different (a-b) outdoor air temperatures, (c-d) outdoor air humidity ratio, and (e-f) dry channel air flowrate.

Eq.3) is assumed to be fixed at 0.65 under all the operating conditions.

Fig. 7(a) shows the percentage of cooling load that is handled by the IEC. The desired supply air condition is assumed to be 20 °C and 9 g/kg. As IEC is suitable for sensible cooling, the percentage is higher when the sensible load is higher, i.e., the outdoor air has higher temperature and lower humidity. When the outdoor humidity ratio is low at 10 g/kg, IEC is able to deal with 70–77% of the overall cooling load. With the increase of outdoor humidity ratio to 15 g/kg, the percentage of cooling load that is undertaken by IEC decreases to 45–58%. The value further drops to 34–48% when the outdoor humidity ratio is 20 g/kg.

With different percentages of cooling load undertaken by IEC, the overall system COP is also different. When the outdoor air is dry, the overall energy efficiency is dominated by the COP of IEC. Therefore, the higher the outdoor temperature, the higher the overall COP, as plotted in Fig. 7(b). In contrast, the COP of standalone MVC, as plotted by the dashed line, decreases with higher outdoor temperatures, as the refrigerant has to be compressed to a higher pressure for heat rejection. The COP of the hybrid IEC-MVC is 39–135% higher than that of a standalone MVC under a low outdoor humidity ratio of 10 g/kg.

When the outdoor humidity ratio is higher at 15 g/kg, more cooling

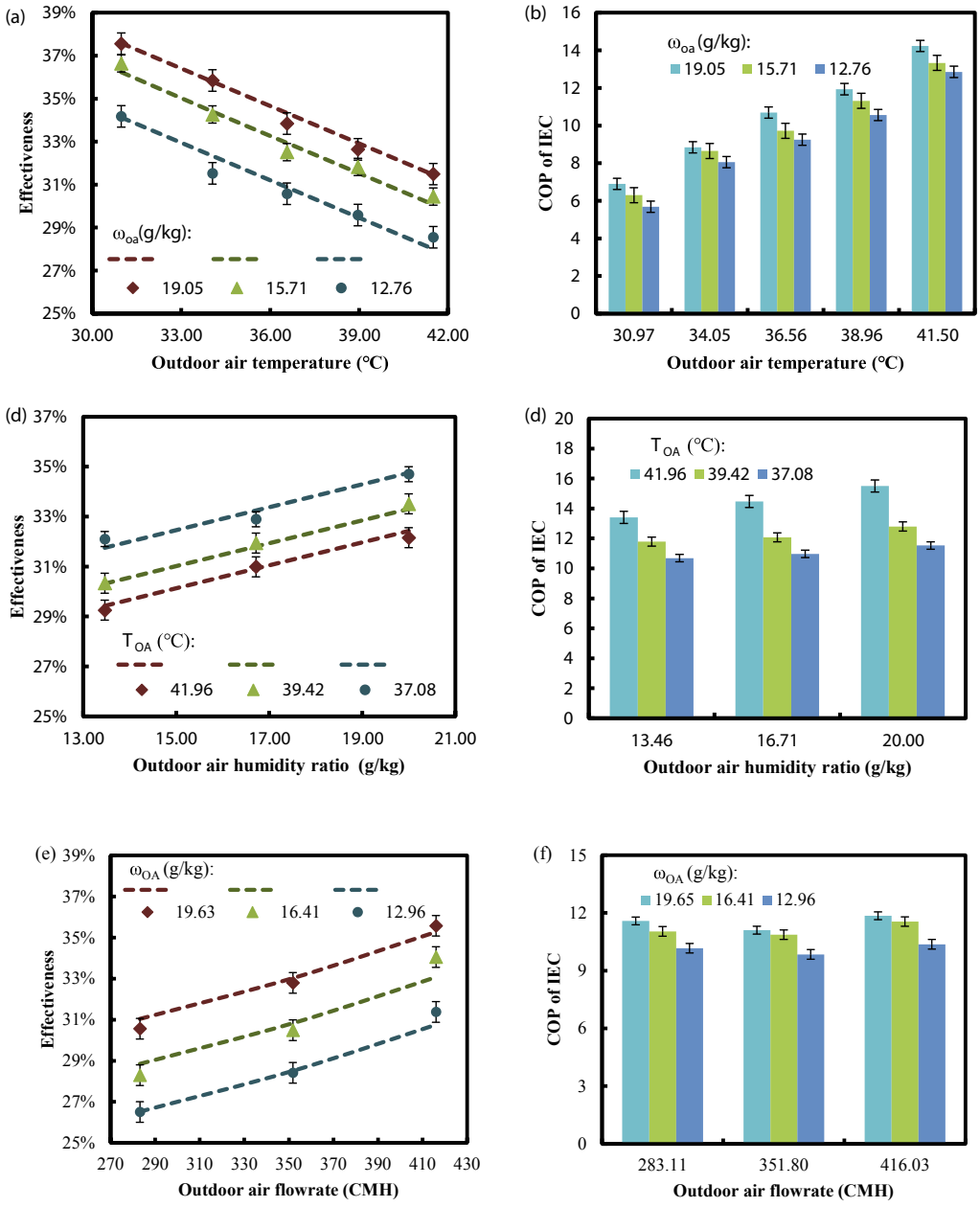

Fig. 6. Enthalpy recovery effectiveness and COP of IEC under different (a-b) outdoor air temperatures, (c-d) outdoor air humidity ratio, and (e-f) dry channel air flowrate.

Table 4
Regression results and statistics for each parameter.

Parameter	Value	Standard error	t-Value	Prob > t
Intercept	0.416	1.55×10^{-2}	26.90	0
T_{OA}	-5.81×10^{-3}	2.85×10^{-4}	−20.37	0
ω_{OA}	4.65×10^{-3}	2.67×10^{-4}	17.40	0
T_{RA}	1.42×10^{-3}	6.11×10^{-4}	2.33	0.02253
ω_{RA}	-5.65×10^{-3}	6.22×10^{-4}	−9.07	5.15×10^{-14}
$\dot{m}_{oa}/\dot{m}_{ra}$	7.49×10^{-4}	3.59×10^{-5}	20.85	0

load has to be handled by MVC. In this case, the overall COP changes marginally with temperature, which is a result of the completing effects between IEC and MVC. The improvement over standalone MVC reduces to 24–79%, which is still significant. The overall COP starts to drop with outdoor temperature when the outdoor humidity ratio is higher at 20 g/kg, while the values are still 19–59% higher than that of standalone MVC.

5. Conclusions

A hybrid indirect evaporative cooling-mechanical vapor compression (IEC-MVC) process is evaluated experimentally and analytically. A cross-flow IEC unit is firstly designed and tested using the room air as the working air in the wet channels, and the energy recovery performance is measured under assorted operating conditions. Afterward, the energy-saving potential of the hybrid IEC-MVC process is analyzed. Key findings of this study are summarized as follows:

(1) IEC is able to recover energy from the room exhaust air to cool and dehumidify the outdoor air. Under the operating ranges

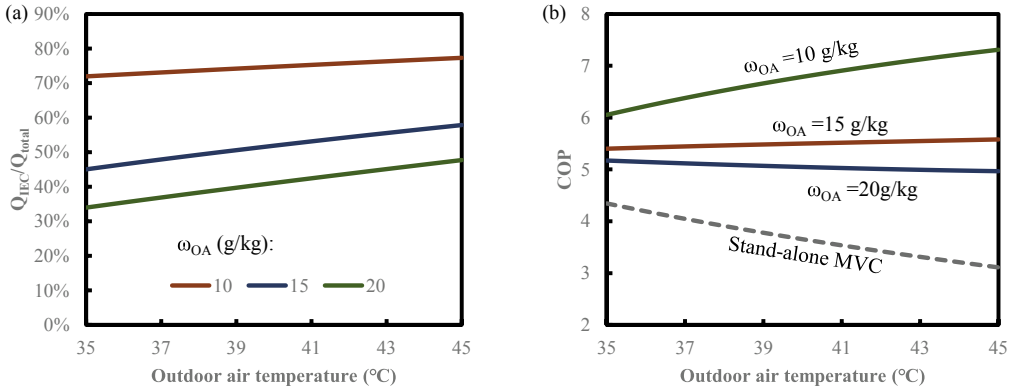

Fig. 7. (a) Ratio of IEC cooling load to total cooling load; (b) COP of IEC-MVC and MVC under different outdoor temperatures and humidity ratios.

considered, the outdoor air temperature and humidity ratio can be reduced by 6–15 °C and 0.5–4 g/kg, respectively;

(2) The effectiveness of enthalpy recovery is in the range of 27–36%. Its value is promoted by lower outdoor temperature, higher outdoor humidity ratio, and higher air flowrate in the dry channels;

(3) The energy efficiency of IEC, expressed as the coefficient of performance (COP), is in the range of 6–16. A higher COP value is observed under a higher outdoor air temperature and humidity ratio;

(4) The percentage of cooling load that can be handled by IEC varies between 34 and 77%. The value is higher when the outdoor air is hot and dry;

(5) Compared with a standalone MVC, the hybrid IEC-MVC process benefits from the high COP of IEC. The overall COP of IEC-MVC can reach 4.96–6.05, 19–135% higher than that of a standalone MVC.

CRediT authorship contribution statement

Qian Chen: Conceptualization, Methodology, Formal analysis, Writing - original draft. **M. Kum Ja:** Methodology, Software, Validation, Investigation. **Muhammad Burhan:** Validation, Formal analysis. **Faheem Hassan Akhtar:** Visualization, Formal analysis. **Muhammad Wakil Shahzad:** Formal analysis. **Doskhan Ybyraiymkul:** Formal analysis. **Kim Choon Ng:** Writing - review & editing, Supervision, Project administration, Funding acquisition.

Declaration of Competing Interest

The authors declare that they have no known competing financial interests or personal relationships that could have appeared to influence the work reported in this paper.

Acknowledgement

This research was supported by the Water Desalination and Reuse Center (WDRC), King Abdullah University of Science and Technology (KAUST).

References

[1] Statistics, I., Key world energy statistics. Paris. International Energy Agency; 2014.
[2] Birol F. The future of cooling: opportunities for energy-efficient air conditioning. Int Energy Agency 2018.
[3] Duan Zhiyin, Zhan Changhong, Zhang Xingxing, Mustafa Mahmud, Zhao Xudong, Alimohammadisagvand Behrang, et al. Indirect evaporative cooling: Past, present and future potentials. Renew Sustain Energy Rev 2012;16(9):6823–50.
[4] Jradi M, Riffat S. Experimental and numerical investigation of a dew-point cooling system for thermal comfort in buildings. Appl Energy 2014;132:524–35.
[5] Dizaji HS, Hu EJ, Chen L, Pourhedayat S. Analytical/experimental sensitivity study of key design and operational parameters of perforated Maisotsenko cooler based on novel wet-surface theory. Appl Energy 2020;262:114557.
[6] Cui X, Islam MR, Mohan B, Chua KJ. Developing a performance correlation for counter-flow regenerative indirect evaporative heat exchangers with experimental validation. Appl Therm Eng 2016;108:774–84.
[7] Heidarinejad Ghassem, Moshari Shahab. Novel modeling of an indirect evaporative cooling system with cross-flow configuration. Energy Build 2015;92:351–62.
[8] Cui X, Chua KJ, Islam MR, Yang WM. Fundamental formulation of a modified LMTD method to study indirect evaporative heat exchangers. Energy Convers Manage 2014;88:372–81.
[9] Anisimov Sergey, Pandelidis Demis, Danielewicz Jan. Numerical analysis of selected evaporative exchangers with the Maisotsenko cycle. Energy Convers Manage 2014;88:426–41.
[10] Zhu Guangya, Chow Tin-Tai, Lee CK. Performance analysis of counter-flow regenerative heat and mass exchanger for indirect evaporative cooling based on data-driven model. Energy Build 2017;155:503–12.
[11] Li Wu-Yan, Li Yong-Cai, Zeng Li-yue, Lu Jun. Comparative study of vertical and horizontal indirect evaporative cooling heat recovery exchangers. Int J Heat Mass Transf 2018;124:1245–61.
[12] Cui X, Chua KJ, Yang WM, Ng KC, Thu K, Nguyen VT. Studying the performance of an improved dew-point evaporative design for cooling application. Appl Therm Eng 2014;63(2):624–33.
[13] Duan Zhiyin, Zhan Changhong, Zhao Xudong, Dong Xuelin. Experimental study of a counter-flow regenerative evaporative cooler. Build Environ 2016;104:47–58.
[14] Al-Zubaydi Ahmed Y Taha, Hong Guang. Experimental study of a novel water-spraying configuration in indirect evaporative cooling. Appl Therm Eng 2019;151:283–93.
[15] Ali M, Ahmad W, Sheikh NA, Ali H, Kousar R, ur Rashid T. Performance enhancement of a cross flow dew point indirect evaporative cooler with circular finned channel geometry. J Build Eng 2021;35:101980.
[16] Moshari Shahab, Heidarinejad Ghassem, Fathipour Aida. Numerical investigation of wet-bulb effectiveness and water consumption in one-and two-stage indirect evaporative coolers. Energy Convers Manage 2016;108:309–21.
[17] Shahzad MW, Burhan M, Ybyraiymkul D, Oh SJ, Ng KC. An improved indirect evaporative cooler experimental investigation. Appl Energy 2019;256:113934.
[18] Shahzad MW, Lin J, Xu BB, Dala L, Chen Q, Burhan M, et al. A spatiotemporal indirect evaporative cooler enabled by transiently interceding water mist. Energy 2021;217:119352.
[19] Wan Y, Huang Z, Soh A, Cui X, Chua KJ. Analysing the transport phenomena of novel dew-point evaporative coolers with different flow configurations considering condensation. Int J Heat Mass Transf 2021;170:120991.
[20] Duan Zhiyin, Zhao Xudong, Zhan Changhong, Dong Xuelin, Chen Hongbing. Energy saving potential of a counter-flow regenerative evaporative cooler for various climates of China: Experiment-based evaluation. Energy Build 2017;148:199–210.
[21] Fikri B, Sofia E, Putra N. Experimental analysis of a multistage direct-indirect evaporative cooler using a straight heat pipe. Appl Therm Eng 2020;171:115133.
[22] Wang Fenghao, Sun Tiezhu, Huang Xiang, Chen Yi, Yang Hongxing. Experimental research on a novel porous ceramic tube type indirect evaporative cooler. Appl Therm Eng 2017;125:1191–9.
[23] Heidari Amirreza, Roshandel Ramin, Vakiloroaya Vahid. An innovative solar assisted desiccant-based evaporative cooling system for co-production of water and cooling in hot and humid climates. Energy Convers Manage 2019;185:396–409.
[24] Pandelidis Demis, Anisimov Sergey, Worek William M, Drag Paweł. Comparison of desiccant air conditioning systems with different indirect evaporative air coolers. Energy Convers Manage 2016;117:375–92.
[25] Cui X, Islam MR, Mohan B, Chua KJ. Theoretical analysis of a liquid desiccant based indirect evaporative cooling system. Energy 2016;95:303–12.
[26] Cui Xin, Liu Yanhua, Liu Yilin, Jin Liwen, Zhao Min, Meng Xiangzhao. Studying the performance of a liquid desiccant indirect evaporative cooling system. Energy Procedia 2019;158:5659–65.

[27] Xiao L, Yang M, Yuan W-Z, Huang S-M. Performance characteristics of a novel internally-cooled plate membrane liquid desiccant air dehumidification system. Appl Therm Eng 2020;172:115193.
[28] Chen Q, Kum Ja M, Li Y, Chua KJ. Thermodynamic optimization of a vacuum multi-effect membrane distillation system for liquid desiccant regeneration. Appl Energy 2018;230:960–73.
[29] Duan Zhiyin, Zhao Xudong, Liu Jingjing, Zhang Qunli. Dynamic simulation of a hybrid dew point evaporative cooler and vapour compression refrigerated system for a building using EnergyPlus. J Build Eng 2019;21:287–301.
[30] Delfani Shahram, Esmaeelian Jafar, Pasdarshahri Hadi, Karami Maryam. Energy saving potential of an indirect evaporative cooler as a pre-cooling unit for mechanical cooling systems in Iran. Energy Build 2010;42(11):2169–76.
[31] Zanchini Enzo, Naldi Claudia. Energy saving obtainable by applying a commercially available M-cycle evaporative cooling system to the air conditioning of an office building in North Italy. Energy 2019;179:975–88.
[32] Cui X, Islam MR, Chua KJ. An experimental and analytical study of a hybrid air-conditioning system in buildings residing in tropics. Energy Build 2019;201:216–26.
[33] Cui X, Chua KJ, Islam MR, Ng KC. Performance evaluation of an indirect pre-cooling evaporative heat exchanger operating in hot and humid climate. Energy Convers Manage 2015;102:140–50.
[34] Chen Yi, Yang Hongxing, Luo Yimo. Parameter sensitivity analysis and configuration optimization of indirect evaporative cooler (IEC) considering condensation. Appl Energy 2017;194:440–53.
[35] Chen Yi, Luo Yimo, Yang Hongxing. A simplified analytical model for indirect evaporative cooling considering condensation from fresh air: Development and application. Energy Build 2015;108:387–400.
[36] Min Y, Chen Y, Yang H. A statistical modeling approach on the performance prediction of indirect evaporative cooling energy recovery systems. Appl Energy 2019;255:113832.
[37] Min Yunran, Chen Yi, Yang Hongxing. Numerical study on indirect evaporative coolers considering condensation: A thorough comparison between cross flow and counter flow. Int J Heat Mass Transf 2019;131:472–86.
[38] Chen Q, Burhan M, Shahzad MW, Ybyraiymkul D, Akhtar FH, Ng KC. Simultaneous production of cooling and freshwater by an integrated indirect evaporative cooling and humidification-dehumidification desalination cycle. Energy Convers Manage 2020;221:113169.
[39] Chen Yi, Yang Hongxing, Luo Yimo. Indirect evaporative cooler considering condensation from primary air: Model development and parameter analysis. Build Environ 2016;95:330–45.
[40] Algorithm (Multiple Linear Regression) - Origin Lab, https://www.originlab.com/doc/origin-help/multi-regression-algorithm.